Numerical Modeling of Marine Seismology in the Arctic Region During Deposit Dissolution due to Oil Migration

Evgeniya K. Guseva[1] (iD)*, Vasily I. Golubev*[1,2] (iD)*, Igor B. Petrov*[1,2] (iD)

As the Arctic region requires costly and difficult to access surveys of the ground, numerical modeling proves to be an effective way to study occurring processes in the area. Moreover, the simulations of the seismic exploration can help identify the main signs of oil migration which is crucial for the risk assessment of the deposit development. Therefore, the main goal of this work is to conduct the forward modeling of the seismology in the offshore areas of the region in order to determine the indicators of such processes. The present study, in particular, is aimed at recreating of basic features of the region such as a layered ground with the gradual change in material parameters and inclusion of a permafrost sheet. Furthermore, the boundaries between layers are considered to be curvilinear. This complex problem was effectively solved using the grid-characteristic method which allows for the accelerating of the calculations using OpenMP. As a result of the computations, the reconstructed wave phenomena is analyzed based on the obtained wave patterns and synthesized seismograms. The change in the responses from the oil reservoir in the process of draining is identified which can further help interpret real measurements.

Keywords: numerical modeling, oil migration, marine seismology, grid-characteristic method, Arctic region.

Introduction

Throughout the years, numerical modeling proved to be a great way to investigate natural and anthropogenous processes, especially in the places of costly and difficult to access in situ measurements such as the Arctic region [11, 15]. The area draws a lot of attention of the researchers due to the significant mineral reserves and promising oil development. This proves the necessity for conducting full-scale surveys of the subsurface areas of ground. For this purpose, measurements are commonly conducted using seismology [23]. Harsh environmental conditions incentify thorough investigation of the area before the preparations for the development of the deposit can begin. Thus, it is essential to identify potential dissolution of the oil-bearing formation which is still a poorly understood mechanism [1, 3]. As a result, numerical modeling can help determine the indicators of this process in the obtained measurements which is the purpose of this work.

However, this task is complicated by the series of unique qualities of the Arctic region which are mainly defined by cold temperatures. As a result, one of the main characteristics of the region is the presence of permafrost sheets, formed when the temperature constantly stays less than $0°C$ for a long period (from a couple to thousands of years) [20]. The layered ground is often inhomogeneous which causes the inconstancy of its mechanical characteristics and the curvilinear boundaries between the sheets. In order to account for the gradual change of the parameters, in this work, the obtained in situ data [14, 16, 26] is used to determine their dependencies on the depth. As a result, the computational domain was introduced consisting of the sea, water floor, permafrost sheet and bottom dense clay layer which contained the oil reservoir that decreased in size due to drain. This distinguishes the study from the previous works that use simpler settings with constant parameters [2, 8] and linear boundaries between the layers [9, 18].

---

[1]Moscow Institute of Physics and Technology, Dolgoprudny, Russian Federation
[2]Scientific Research Institute for System Analysis of the National Research Centre "Kurchatov Institute", Moscow, Russian Federation

The computer modeling was conducted using a software package RECT written in C++ and dedicated to the solution of hyperbolic equations by applying the grid-characteristic method [5] on structured grids. This method allows for effective solution of dynamic problems in objects of complex shapes [6] and with different rheologies [7]. Moreover, the software supports several means of parallelization, such as OpenMP [13], MPI [19], and CUDA [12] with the former one used to accelerate calculations in this work. The package is developed by the Computational Physics Department and the Informatics and Computational Mathematics Department of the Moscow Institute of Physics and Technology. The article is organized as follows. Section 1 is devoted to explanation of numerical setting including the governing system of equations in Section 1.1, computational method in Section 1.2 and domain in Section 1.3. Obtained results are discussed in Section 2, they consist of the wave patterns analyzed in Section 2.1 and seismograms in Section 2.2. Conclusion summarizes the study and points directions for further work.

1. Numerical Setting

1.1. Governing System of Equations

In order to represent all layers of the computational domain, isotropic linear elasticity is used. In the current work, the simulations are conducted in two-dimensional case. Three-dimensional calculations require a lot of time and computational resources while showing results similar to the plane problem [24]. The difference between these settings can be the result of the strong asymmetry which is not considered in this work. Thus, it is still possible to determine the influence of the deposit dissolution on the seismic measurements. The governing system of equations can be written in the following form:

$$
\begin{aligned}
\rho \frac{\partial v_x}{\partial t} &= \frac{\partial \sigma_{xx}}{\partial x} + \frac{\partial \sigma_{yx}}{\partial y} + f_x, \\
\rho \frac{\partial v_y}{\partial t} &= \frac{\partial \sigma_{xy}}{\partial x} + \frac{\partial \sigma_{yy}}{\partial y} + f_y, \\
\frac{\partial \sigma_{xx}}{\partial t} &= (\lambda + 2\mu)\frac{\partial v_x}{\partial x} + \lambda\frac{\partial v_y}{\partial y}, \\
\frac{\partial \sigma_{yy}}{\partial t} &= \lambda\frac{\partial v_x}{\partial x} + (\lambda + 2\mu)\frac{\partial v_y}{\partial y}, \\
\frac{\partial \sigma_{xy}}{\partial t} &= \mu\left(\frac{\partial v_x}{\partial y} + \frac{\partial v_y}{\partial x}\right).
\end{aligned}
\tag{1}
$$

Here the velocity vector of medium points $\mathbf{v} = (v_x, v_y)^\intercal$ and the stress tensor σ are unknown and calculated after each time step. The material parameters are density ρ and Lame parameters λ and μ, the equations also allow for introduction of external forces $\mathbf{f} = (f_x, f_y)^\intercal$. This model reconstructs pressure and shear waves with velocities $c_p = \sqrt{\frac{\lambda+2\mu}{\rho}}$ and $c_s = \sqrt{\frac{\mu}{\rho}}$. These velocities and density fully define these equations.

1.2. Grid-Characteristic Method

For the solution of the hyperbolic problem (1), the grid-characteristic method [5] is used. According to the procedure, the initial system is rewritten with introduction of the new vector of unknowns $\mathbf{u} = (v_x, v_y, \sigma_{xx}, \sigma_{yy}, \sigma_{xy})^\intercal$:

$$
\frac{\partial \mathbf{u}}{\partial t} + A_x \frac{\partial \mathbf{u}}{\partial x} + A_y \frac{\partial \mathbf{u}}{\partial y} = \mathbf{g}.
\tag{2}
$$

Here matrices A_i are introduced:

$$A_x = - \begin{pmatrix} 0 & 0 & 1/\rho & 0 & 0 \\ 0 & 0 & 0 & 0 & 1/\rho \\ \lambda + 2\mu & 0 & 0 & 0 & 0 \\ \lambda & 0 & 0 & 0 & 0 \\ 0 & \mu & 0 & 0 & 0 \end{pmatrix}, \; A_y = - \begin{pmatrix} 0 & 0 & 0 & 0 & 1/\rho \\ 0 & 0 & 0 & 1/\rho & 0 \\ 0 & \lambda & 0 & 0 & 0 \\ 0 & \lambda + 2\mu & 0 & 0 & 0 \\ \mu & 0 & 0 & 0 & 0 \end{pmatrix}. \tag{3}$$

Next, coordinate-wise splitting and splitting on physical processes are performed. At first, the step along the horizontal axis x is calculated, next, the step along the vertical axis y was made. Finally, external forces were taken into account. For the solution of each of these equations, the new variables, Riemann invariants $\mathbf{r}_i = \{r_i^j\}_{j=1}^5$, were introduced. As the system (2) is hyperbolic, matrices A_i, $i = \{x, y\}$ can be presented in the form $A_i = R_i \Lambda_i L_i$, where L_i is the eigenvector matrix, $R_i = L_i^{-1}$, and $\Lambda_i = diag\{0, -c_s, c_s, -c_p, c_p\}$ is the eigenvalue matrix. Thus, (2) can be rewritten as the system of one-dimensional transport equations with $\mathbf{r}_i = L_i \mathbf{u}$:

$$\frac{\partial \mathbf{r}_i}{\partial t} + \Lambda_i \frac{\partial \mathbf{r}_i}{\partial i} = 0. \tag{4}$$

For the solution of each equation in (4), third order Rusanov scheme was applied [21], monotonized using the grid-characteristic monotonicity criterion [10]:

$$[r_i^j]_m^{n+1} = [r_i^j]_m^n + \frac{c_i^j}{2}([r_i^j]_{m-1}^n - [r_i^j]_{m+1}^n) + \frac{c_i^{j\,2}}{2}([r_i^j]_{m-1}^n - 2[r_i^j]_m^n + [r_i^j]_{m+1}^n) -$$
$$- \frac{c_i^j(1 - c_i^{j\,2})}{6}([r_i^j]_{m-2}^n - 3[r_i^j]_{m-1}^n + 3[r_i^j]_m^n - [r_i^j]_{m+1}^n).$$

Here the Courant number is introduced $c_i^j = \frac{\lambda_i^j \tau}{h_i}$, and $j \in [1, 5]$, λ_i^j is the corresponding eigenvalue, h_i is the spacial step. Condition $c_i^j < 1$ guaranteed the stability of the calculations. One of the numerical problems which is common of the dynamic processes in the layered media is the appearance of non-physical oscillations due to high gradients in the mechanical properties. To deal with this issue, we introduce the grid-characteristic criterion in order to monotonize the solution. When $[r_i^j]_m^{n+1} \le \min{[r_i^j]_1^n, [r_i^j]_2^n}$, the following correction was performed: $[r_i^j]_m^{n+1} = \min{[w_i^j]_1^n, [r_i^j]_2^n}$. In case $[r_i^j]_m^{n+1} \ge \max{[r_i^j]_1^n, [r_i^j]_2^n}$, another formulae was used: $[r_i^j]_m^{n+1} = \max\{[r_i^j]_1^n, [r_i^j]_2^n\}$. Here $[r_i^j]_1^n$, $[r_i^j]_2^n$ are the grid function values at the time $t = t_n$ in the nearest points to the characteristic which originates from the point (t_n, x_m). The introduced scheme is explicit which made it possible to employ parallelism using the OpenMP technology. This allowed for the significant acceleration of the calculations.

1.3. Computational Domain

In order to conduct simulations, the computational domain in a two-dimensional case was created. It consisted of the around 100 m deep sea layer, and about 100 m wide seabed, 300 m wide permafrost and a deepest dense soil sheet beneath it. The bottom layer contained an oil deposit, which was gradually draining due to oil migration [1]. The layout for the problem is presented in Fig. 1. The widths of the layers correspond to the mean values, registered in this geographical region. The boundaries between all areas were significantly curvilinear. The dissolution of the reservoir was represented as the gradual change of its size.
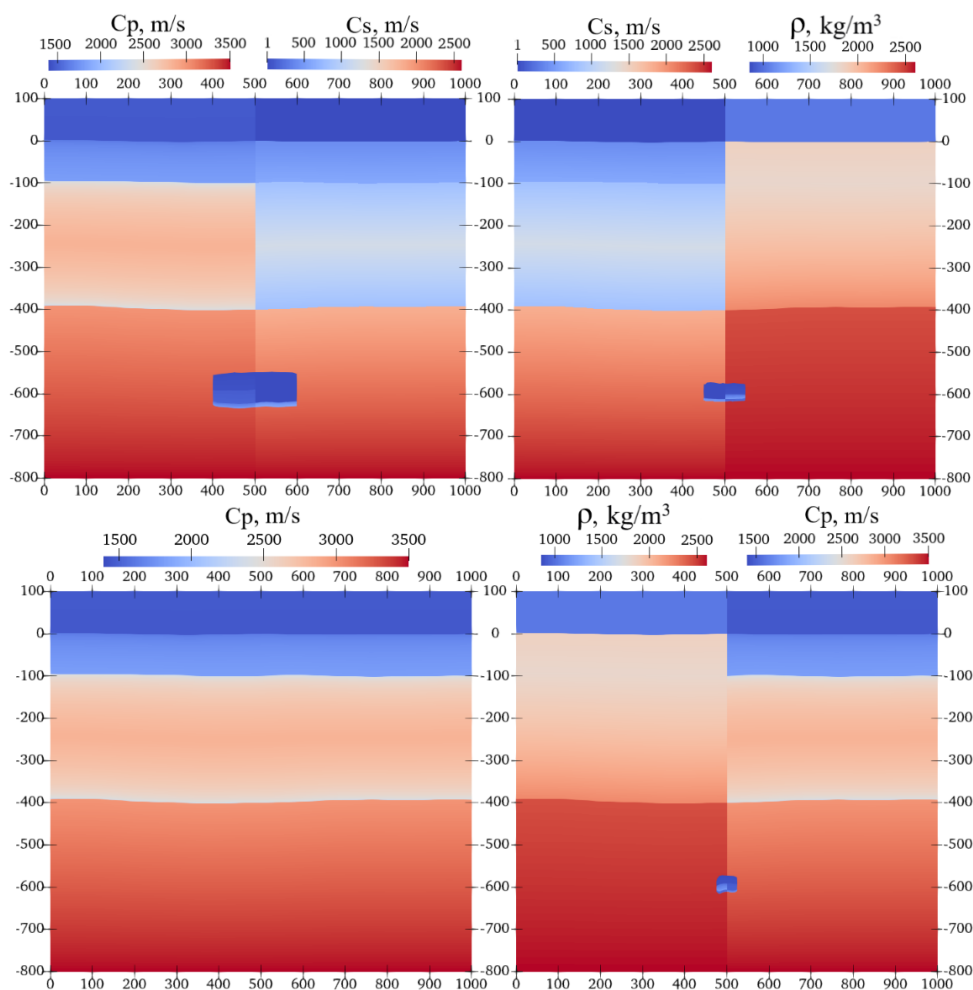
Figure 1. Layout of the computational domain and elastic parameters of layers

1.3.1. Material parameters

To construct an adequate geological model, the ground was considered to be a vertically inhomogeneous medium. The dependencies of the elastic parameters on depth obtained from the experimental data [16] were used as a basis for formulation of the gradient corresponding to each layer. All parameters remained within their characteristic values as noted in [16, 26]. The final relations between the elastic parameters and the depth are presented in Figs. 2–3. In the water layer, the change in the velocity of the pressure waves is associated with the temperature gradient, often observed in the northern seas [14]. Thus, the pressure wave velocity changed according to the similar trend. Moreover, in this layer, the density was equal to 1024 kg/m^3, and the shear wave velocity was set to 1 m/s.

Under the water, the transition from the thawed soil of the seabed to the frozen soil of the permafrost layer was reproduced based on a gradual decrease in temperature. However, as the temperature rises and stabilizes, the permafrost ends with a transition to a denser clay layer, which was reflected in the density change. For the velocities of the pressure waves, a standard power-law change in parameters at shallow depths was set. For greater depths, a linear increase was used. Additionally, the shear wave velocity and density were changed linearly. The drying of the deposit was modeled by a successive size reduction of the oil reservoir. Inside it, a small

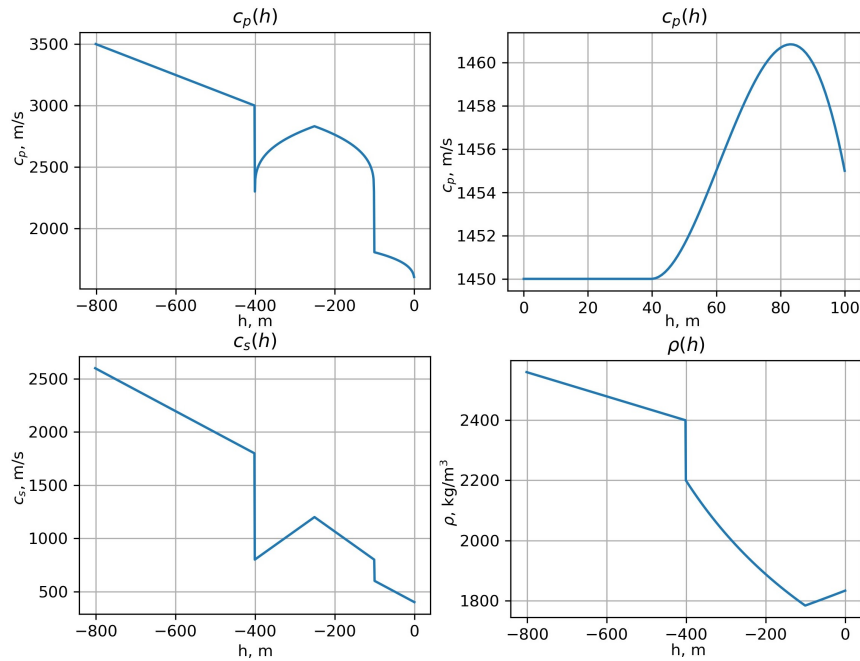transition was considered from the upper oil layer to the water base and the thawed bottom of the reservoir.

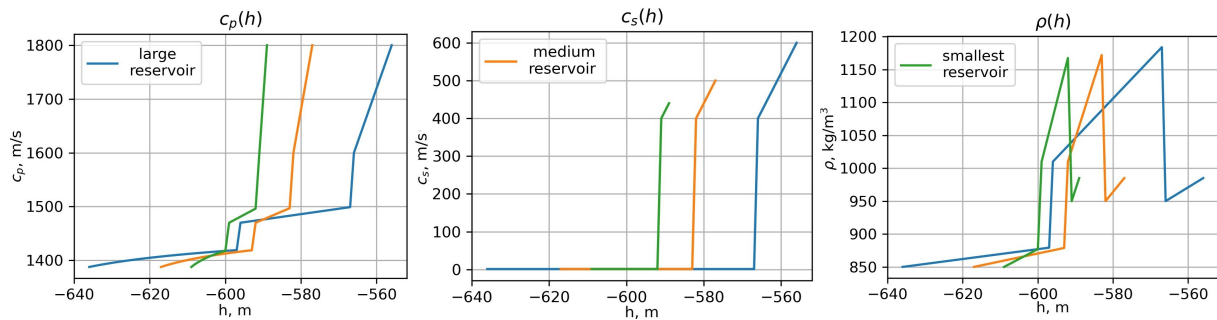**Figure 2.** Elastic parameters in water and soil without a reservoir along the depth

Figure 3. Elastic parameters in a reservoir along the depth: oil layer on the surface of water and wet soil

1.3.2. Grid parameters

There are two basic approaches to creation of computational grids. The first one consists of using explicit contact conditions and creating grids for each area of the domain. According to the second approach, one rectangular grid is created and in each node corresponding material parameters are set. Both approaches allow for reproducing of all wave fronts and results in similar wave patterns [8, 25], however, both also have downfalls.

The second method is characterized by an increase in the amplitude of individual waves. There may also be a lack of smoothness in the incoming signals due to the step-wise nature of the sections of geological media. For the first method, it is necessary to create curvilinear grids, which, if constructed incorrectly, can distort the shape of the wave fronts. Additional numerical errors can also be introduced by nonphysical boundaries within layers with inclusions

when constructing structured grids. Such effects lead to the inability to compute the difference between results obtained in different setups. This is a significant drawback as this technique is often used for analyzing processes in dynamics, and is also employed in this work.

Moreover, the gradual nature of elastic parameters of the layers incentifies the usage of the second approach. Thus, in order to save time, computational resources and make it easier to set material parameters, one rectangular grid of 1000×900 cells was created. In order to account for the curvilinear boundaries, the dependencies in Figs. 2–3 were interpolated on the grid for each layer separately. Therefore, in each node, the elastic parameters of the corresponding areas were set. To fulfill the Courant stability condition, the time step was set equal to 0.1 ms. The total calculation time was 1 s. The top boundary of the domain was considered to be free, on the other sides, characteristic absorbing conditions were placed. The seismic point source was described as the 30 Hz Ricker pulse. Two different signal generator's positions were compared: on the water surface and on the seabed. The receivers were placed on the water surface and on the seabed with the 2 m horizontal spacing.

2. Simulation Results

As a result of the calculations, spatial wave fields and synthetic seismograms were produced (see Figs. 4–6).

2.1. Wave Patterns

The wave pattern analysis shows that the wave fronts generated by both sources are similar to each other. However, it is noticeable that when the source position is set on the sea surface, the amplitude of some waves decreases. This is related to the fact that, as water is an acoustic medium, it partially absorbs some waves. Moreover, this is also the reason why there are no surface waves, such as Rayleigh waves [17], observed on the upper boundary. However, when the source is located on the seabed, surface Stoneley (also called Scholte) waves [22] appear and propagate along the water floor.

As the position of the source at the seabed is closer to the reservoirs, the initial wave reaches the deposit earlier. Nonetheless, in both cases, while propagating through the stratified medium, this wave undergoes multiple reflections. Moreover, the gradient of elastic parameters seem to result in appearance of additional oscillations in the wave. The narrow top layers create a wave channel which leads to the formation of seismic ghost reflections [4] which can conceal the initial wave rebounded from the deposit.

These reflections from the reservoirs are the crucial point of the seismology which help identify the internal processes in the ground such as oil migration. It is worth noting that all such reflections, as shown in Fig. 4, have a similar rounded shape which originate from the borders of the layer. As the deposit dissolves, the shape transforms from the oval to the spherical one. Moreover, when the size of the reservoir decreases, its upper boundary moves farther from the day surface which is indicative of the change in the travel time that can be expected in the considered setting. Overall, curvilinear boundaries account for asymmetry in the resulting pictures.

Additionally, in Fig. 4, several computational artifacts are present. The point signal leaves a noticeable cross-shaped trace in the wave patterns, especially in case of the generator on the water surface. Moreover, non-physical reflections from the sides of the domain can appear due
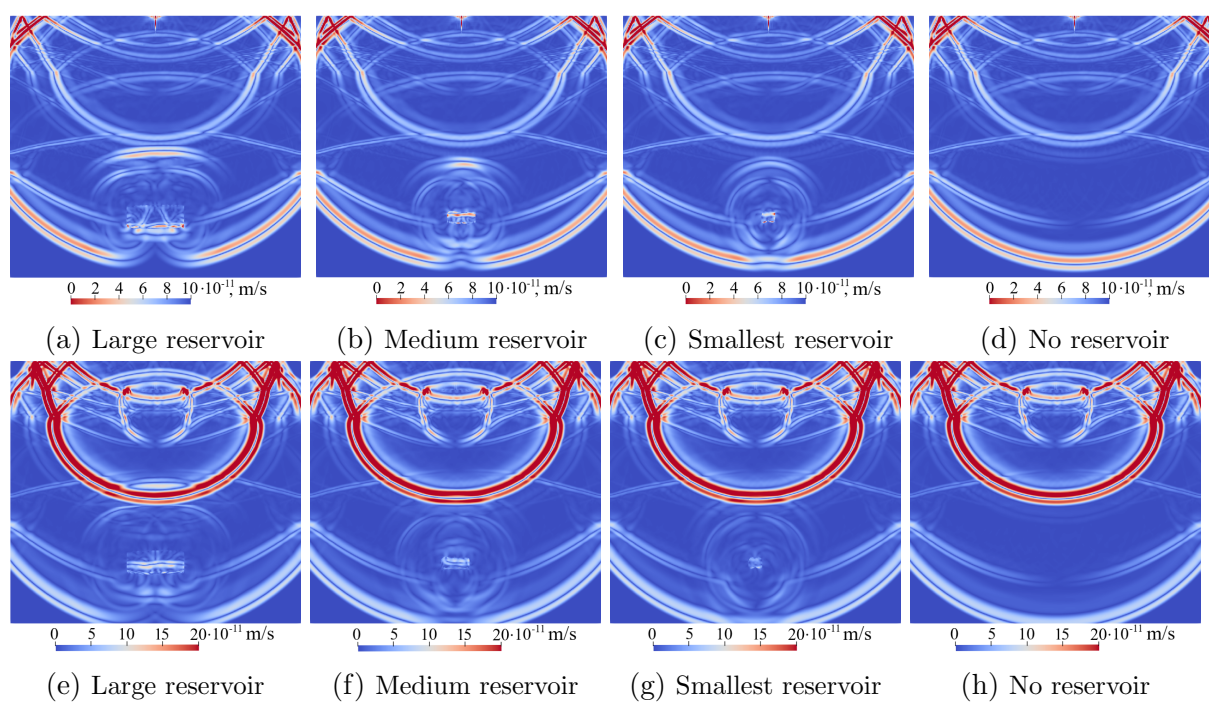
(a) Large reservoir   (b) Medium reservoir   (c) Smallest reservoir   (d) No reservoir

(e) Large reservoir   (f) Medium reservoir   (g) Smallest reservoir   (h) No reservoir

Figure 4. Wave fields. The top row is generated for the source in the water (T = 0.35 s), the bottom row – for the source on the seabed (T = 0.3 s)

to the well known problem of the absorbing boundary conditions. However, these effects do not influence the results significantly.

2.2. Synthesized Seismograms

All of the effects noted in the wave patterns can also be clearly identified in synthetic seismograms (Figs. 5–6). When the position of the sources and the receivers coincide (first and last rows in Fig. 5), the seismograms show the presence of the initial impulse above other signals. Additionally, in case of the source in the seabed (first row), the noted Stoneley surface waves are also present. However, when the signal generator is moved to the water surface, the signs of these waves (third row) can also be seen, although they are not that prominent.

The second most distinguished signals are the first reflections of the initial wave from the water surface and the seabed. These waves are followed by multiple responses formed by the waves' circulation between these boundaries. Thus, seismic ghost reflections [4] produce a lot of noise in the seismograms and make the resulting seismograms almost indistinguishable between each other as the oil deposit drains. Moreover, in case of the placement of the sources and the signal receivers on the same surface, surface waves further conceal the rest of the picture. Therefore, the most convenient position of the receivers should not coincide with the position of the sources.

Additionally, the discovered non-physical reflections from the sides of the domain can also hinder the analysis of the calculations. As a result, the difference between the settings can be noted only about 0.5 s after the calculations in the central parts of each seismogram. Therefore, they require further processing as it is hard to identify oil migration. To solve this problem, the differences between the settings with and without reservoirs were calculated. In practice, in order to trace down the occurring processes, this procedure can be performed after consecutive
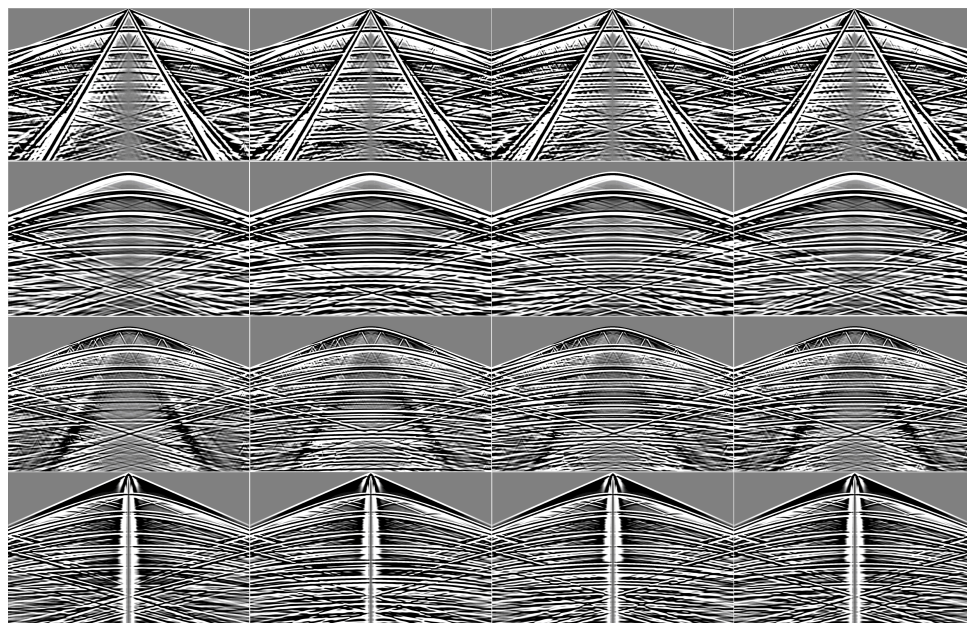
Figure 5. Synthetic seismograms. The top two rows represent the source in the seabed, the bottom two rows – the source on the water. The first and the third rows obtained from the receivers on the seabed, the second and the forth – from the water surface.
The first column corresponds to the case without reservoir, the second one – with the larger reservoir, the third one – with the medium one, the fourth one – with the smallest one

measurements or when the general geometry of the seabed is well-known beforehand. As part of numerical analysis, this technique allows us to investigate the signal from the reservoir separately from other responses.

The resulting seismograms are presented in Fig. 6. The picture shows that the signals of different reservoirs are very similar. In accordance with the wave patterns, the travel time decreases with the placement of sources closer to the oil deposit. Moreover, the dissolution of the reservoirs also results in a slight decrease in the travel time. Another notable difference between the settings previously shown in wave patterns is the change in the form of the reflection from the reservoirs which coincides with the transformation of the shape of the responses on the seismograms. At the same time, it becomes harder to identify the changes as the reservoirs become smaller. So, we can conclude that it is crucial to obtain seismic measurements of the initial state of the oil deposit for further gradual comparisons.

Conclusion

As the result of conducted simulation, the direct problem of marine seismology in the Arctic during oil migration was solved. The distinctive feature of this work is the creation of the computational domain that encompasses the basic features of the offshore areas, including the permafrost ground, and the reflection of gradient change of elastic parameters in the layered ground obtained in real measurements. The usage of the grid-characteristic method allowed for effective solution of problem accelerated by the parallelization using OpenMP. Deposit dissolution was accounted for by the gradual decrease in the size of the reservoir.

Calculated wave patterns and synthesized seismograms not only showed the responses from the reservoir but also demonstrated complex wave phenomena, such as surface waves and seismic
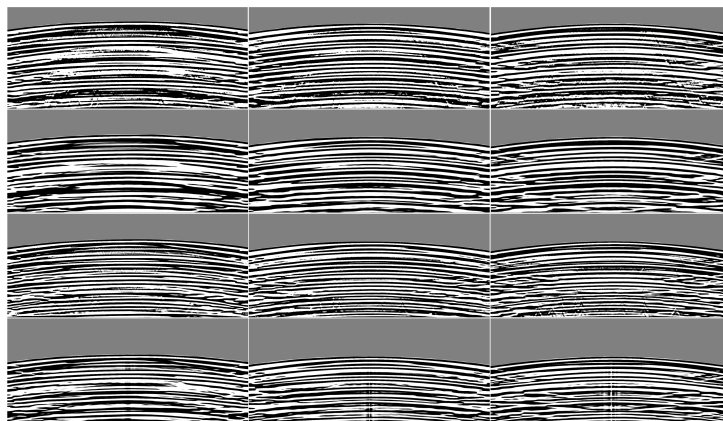
Figure 6. Differences between seismograms with and without oil deposit. The placement of the rows correspond to Fig. 5. The first column represents the setting with the larger reservoir, the second one – with the medium reservoir, the third one – with the smallest reservoir. Top one-third of each picture is not included

ghost reflections. Due to the presence of such waves, the obtained seismograms contain a lot of noise and require further processing. Therefore, in situ measurements should be conducted consecutively to register initial state of the oil deposit for further gradual comparisons. More adequate estimations can be conducted based on the real data and specific deposits. The precise reason for oil migration should also be taken into account, in order to be able to identify particular attributes of the process. Comparison of the results of the simulations in the plane problem to the three-dimensional case can also be noted as the direction for further work.

Acknowledgements

References

1. Beletskaya, S.: Mechanisms and factors of primary oil migration. modeling of primary migration processes (in russian). Oil and Gas Geology. Theory and Practice 2, 28 (2007), `http://www.ngtp.ru/rub/1/028.pdf`

2. Biryukov, V.A., Miryakha, V.A., Petrov, I.B., Khokhlov, N.I.: Simulation of elastic wave propagation in geological media: Intercomparison of three numerical methods. Computational Mathematics and Mathematical Physics 56, 1086–1095 (2016). `https://doi.org/10.1134/s0965542516060087`

3. Chilingar, G., Katz, S., Fedin, L., *et al.*: Primary versus secondary migration of oil. Journal of Sustainable Energy Engineering 2(4), 323–330 (2015). `https://doi.org/10.7569/JSEE.2014.629517`

4. Fatyanov, A.: A wave method of suppressing multiple waves for any complex subsurface geometry. Numerical Analysis and Applications 5, 187–190 (2012). `https://doi.org/10.1134/s1995423912020140`

5. Favorskaya, A.V., Petrov, I.B.: Grid-characteristic method. In: Favorskaya, A., Petrov, I. (eds.) Innovations in Wave Processes Modelling and Decision Making, Smart Innovation, Systems and Technologies, vol. 90, pp. 117–160. Springer, Cham (2018). `https://doi.org/10.1007/978-3-319-76201-2_5`

6. Favorskaya, A.V., Petrov, I.B.: Calculation of seismic stability of buildings in the Far North using the Grid-Characteristic Method. Lobachevskii Journal of Mathematics 45(1), 213–222 (2024). `https://doi.org/10.1134/S1995080224010153`

7. Golubev, V.I., Nikitin, I., Beklemysheva, K.A.: Model of fractured medium and nondestructive control of composite materials. Chinese Journal of Aeronautics 37(2), 93–99 (2024). `https://doi.org/10.1016/j.cja.2023.11.023`

8. Guseva, E.K., Golubev, V.I., Petrov, I.B.: Investigation of wave phenomena during the seismic survey in the permafrost areas using two approaches to numerical modeling. Lobachevskii Journal of Mathematics 45(1), 231–238 (2024). `https://doi.org/10.1134/S1995080224010190`

9. Guseva, E.K., Golubev, V.I., Petrov, I.B.: Investigation of Wave Phenomena in the Offshore Areas of the Arctic Region in the Process of the Seismic Survey. Lobachevskii Journal of Mathematics 45(1), 223–230 (2024). `https://doi.org/10.1134/S1995080224010189`

10. Guseva, E., Golubev, V., Petrov, I.: Linear quasi-monotone and hybrid grid-characteristic schemes for the numerical solution of linear acoustic problems. Numerical Analysis and Applications 16, 112–122 (2023). `https://doi.org/10.1134/S1995423923020027`

11. Henderson, J., Loe, J.S.P.: The prospects and challenges for Arctic oil development. The Oxford Institute for Energy Studies (2014). `https://doi.org/10.26889/9781784670153`

12. Khokhlov, N., Ivanov, A., Zhdanov, M., *et al.*: Applying OpenCL technology for modelling seismic processes using grid-characteristic methods. In: Vishnevskiy, V., Samouylov, K., Kozyrev, D. (eds.) Distributed Computer and Communication Networks. DCCN 2016, Communications in Computer and Information Science, vol. 678, pp. 577–588. Springer, Cham (2016). `https://doi.org/10.1007/978-3-319-51917-3_49`

13. Khokhlov, N.I., Petrov, I.B.: Application of the grid-characteristic method for solving the problems of the propagation of dynamic wave disturbances in high-performance computing systems (in russian). Proceedings of the Institute for System Programming of the RAS (Proceedings of ISP RAS) 31(6), 237–252 (2019). `https://doi.org/10.15514/ispras-2019-31(6)-16`

14. Khutorskoy, M.D., Akhmedzyanov, V.R., Ermakov, A.V., *et al.*: Geothermics of the Arctic seas (in russian). In: Transactions of the Geological Institute, vol. 605. GEOS, Moscow (2013)

15. Kruk, M.N., Nikulina, A.Y.: Economic estimation of project risks when exploring sea gas and oil deposits in the Russian Arctic. International Journal of Economics and Financial Issues 6(2), 138–150 (2016), `https://dergipark.org.tr/tr/pub/ijefi/issue/31980/352620`

16. Nazarov, G.N.: Methodical instructions for complex seismic-geological and engineering-geological studies using portable seismic exploration equipment (in russian). Publishing house VIA, Moscow (1969)

17. Nkemzi, D.: A new formula for the velocity of Rayleigh waves. Wave Motion 6(2), 199–205 (1997). `https://doi.org/10.1016/s0165-2125(97)00004-8`

18. Petrov, D.I., Petrov, I.B., Favorskaya, A.V., Khokhlov, N.I.: Numerical solution of seismic exploration problems in the Arctic region by applying the grid-characteristic method. Computational Mathematics and Mathematical Physics 56, 1128–1141 (2016). `https://doi.org/10.1134/s0965542516060208`

19. Petrov, I.B., Khokhlov, N.I.: Modeling 3D seismic problems using high-performance computing systems. Mathematical Models and Computer Simulations 6, 342–350 (2014). `https://doi.org/10.1134/s2070048214040061`

20. Romanovsky, V.E., Drozdov, D.S., Oberman, N.G., *et al.*: Thermal state of permafrost in Russia. Permafrost Periglac 21, 136–155 (2010). `https://doi.org/10.1002/ppp.683`

21. Rusanov, V.V.: Difference schemes of the third order of accuracy for the forward calculation of discontinuous solutions. Doklady Akademii Nauk 180, 1303–1305 (1968), `https://www.mathnet.ru/eng/dan33936`

22. Scholte, J.: On the Stoneley wave equation. Proceedings of the Koninklijke Nederlandse Akademie van Wetenschappen 45(1), 20–25 (1942)

23. Shearer, P.M.: Introduction to seismology. Cambridge university press (2019). `https://doi.org/10.1017/9781316877111`

24. Stognii, P.V., Khokhlov, N.I., Petrov, I.B.: Numerical modeling of wave processes in multilayered media with gas-containing layers: Comparison of 2D and 3D models. Doklady Mathematics 100, 586–588 (2019). `https://doi.org/10.1134/S1064562419060152`

25. Stognii, P.V., Khokhlov, N.I., Petrov, I.B., Favorskaya, A.: The comparison of two approaches to modeling the seismic waves spread in the heterogeneous 2D medium with gas cavities. In: Favorskaya, M.N., Favorskaya, A.V., Petrov, I.B., Jain, L.C. (eds.) Smart Modelling For Engineering Systems, Smart Innovation, Systems and Technologies, vol. 214, pp. 101–114. Springer, Cham (2021). `https://doi.org/10.1007/978-981-33-4709-0_9`

26. Trifonov, B.A., Milanovsky, S.Y., Nesynov, V.V.: Assessment of seismic impacts in conditions of permafrost degradation (in russian). Bulletin of KRAUNC. Series: Earth Sciences 56(4), 59–74 (2022). `https://doi.org/10.31431/1816-5524-2022-4-56-59-74`